

2022 GO-SHIP P2 LADCP Post-Cruise QC Report

A.M. Thurnherr

May 11, 2023

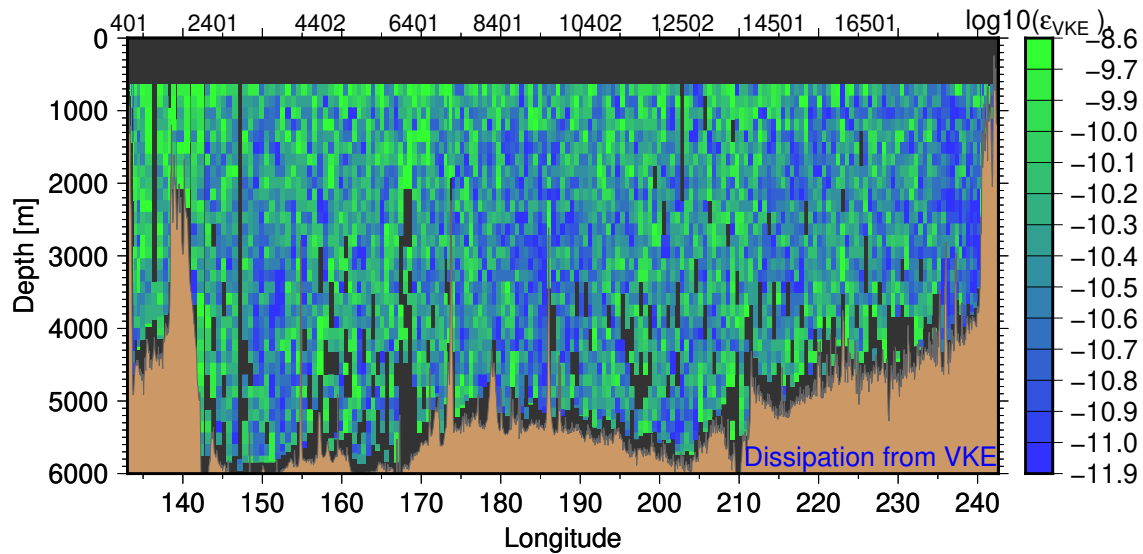


Figure 1: Kinetic energy dissipation in units of $W \cdot kg^{-1}$ along P2 from a finescale parameterization based on vertical kinetic energy (ϵ_{VKE}). This figure was created from the default output of the LADCP_w software, version 2.1, applied to the P2 LADCP data, without any manual filtering or modification of the default processing parameters.

1 Summary

This report describes the results from the post-cruise quality control of the LADCP data collected during both legs of the 2022 GO-SHIP re-occupation of the P2 repeat hydrography section with the UNOLS vessel R/V *Roger Revelle*. Using two ADCPs installed on the CTD rosette, one looking downward (DL) and the other upward (UL), full-depth profiles of all three components of the oceanic velocity field were collected. Additional “bio casts” to 1000 m were collected nominally at every 3rd station. Additional information about the LADCP data acquisition logistics on this cruise can be found in the LADCP section of the cruise report. The cruise track along $30^\circ N$ crosses the center of

the subtropical gyre, a region with extremely low acoustic backscatter. As a result, there are some gaps in the LADCP vertical-velocity profiles and the instrument range in about 40% of the deep profiles was sufficiently reduced to prevent processing for full depth horizontal velocity.

2 ADCP Instruments and Setup

Overall, the cruise can be split into three groups of profiles:

1. All Leg-1 profiles 00102–11701.
2. The Leg-2 profiles 11801–18601, 18701, 18801, 18802, 18901, 19001, 19101, 19102, and 19201–20401, which complete the P2 section.
3. The remaining Leg-2 profiles 18602, 18702, 18803, 18804, 18902, 19002, 19103, 19104, which make up a partial second crossing of the California Current System.

Five different ADCPs were used during this cruise; all are 300kHz TRDI Workhorse Monitor instruments. The instrument with serial #3441 was used as the downlooker for all profiles, except for the 2nd crossing of the CCS when instrument #24477 was used instead. That latter instrument was outfitted with an experimental self-recording accelerometer/magnetometer/gyro package called IMP Mk3A. Three different ADCPs were used as uplookers. Initially on leg-1 instrument #150 was used (profiles 00102-02901), until it failed on profile 02902. For the remainder of the cruise leg instrument #754 was used. For leg-2 another instrument (serial #12734) with a self-recording IMU (IMP MK3, without gyros) was installed and used throughout.

The standard US GO-SHIP ADCP setup was used on stations 001–079; this setup uses 8 m pulse and bin lengths. The blanking distance is set to zero but the data from the first bin are not used for processing. Because of the poor backscatter environment starting on station 080 the pulse and bin lengths were increased to 10 m and the blanking interval was set to 4 m in an attempt to increase the useful profile range.

3 Sampling Conditions

Figure 2 shows the maximum depths from all profiles. At approximately one third of all stations, a bio-cast to 1000 m was collected first, followed by a full depth “core” cast. Except for the profiles collected over the continental shelves and slopes, as well as a few seamount peaks, most core profiles are very deep, which increases the errors of the resulting horizontal velocities.

The most important parameter affecting the quality of horizontal LADCP velocities is the measurement range of the instrument which, for a given instrument, depends primarily on the acoustic backscatter environment. Along the track of P2 the backscatter environment in the open ocean below about 2000 m is poor with the backscatter dropping below -97 dB, an approximate lower limit for collecting horizontal LADCP velocities with WH300 ADCPs, in the bottom 1000–2000 m in most profiles (Figure 3). [There are indications that the backscatter in some eddies is elevated throughout the full water-column.] Since gap-less profiles are required for full-depth horizontal velocity processing, it is anticipated that there are many partial depth u and v profiles, in particular between 145° and 170° W, as well as east of 195° W (175° E).

Sea state can also affect LADCP data quality with some LADCP installations; in Figure 4 the sea state is quantified as the *rms* vertical package acceleration. Conditions during the cruise were mostly calm (heave acceleration below $0.2 \text{ m}\cdot\text{s}^{-2}$) to very calm (heave acceleration below $0.15 \text{ m}\cdot\text{s}^{-2}$).

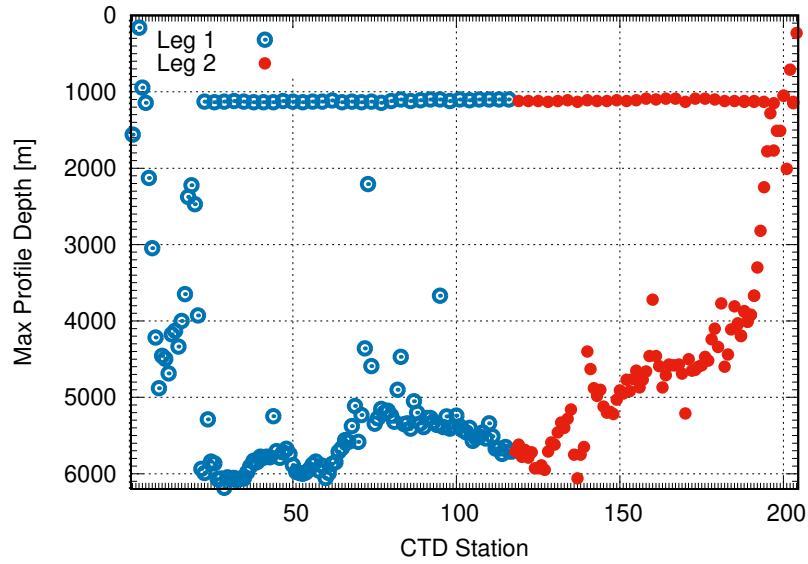


Figure 2: Maximum ADCP profile depths; deep-water profiles to 1000 m are bio-casts.

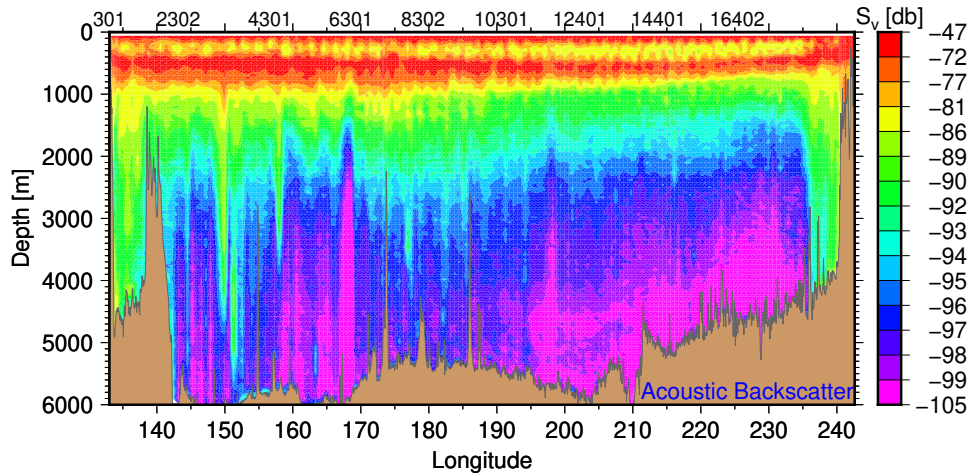


Figure 3: Downcast acoustic backscatter coefficient S_v from the DI data, calculated using the vertical-velocity processing software. Based on the data from previous cruises, the lower limit for collecting LADCP profiles with a dual Workhorse LADCP system is somewhere between ≈ -97 dB and -100 dB.

Package accelerations below $0.1 \text{ m}\cdot\text{s}^{-2}$ are typically only observed when doing CTD work in regions with heavy sea-ice cover.

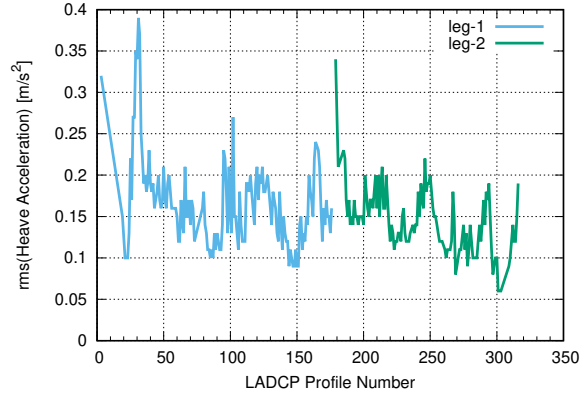


Figure 4: *Rms* vertical acceleration due to vessel heave (sea state).

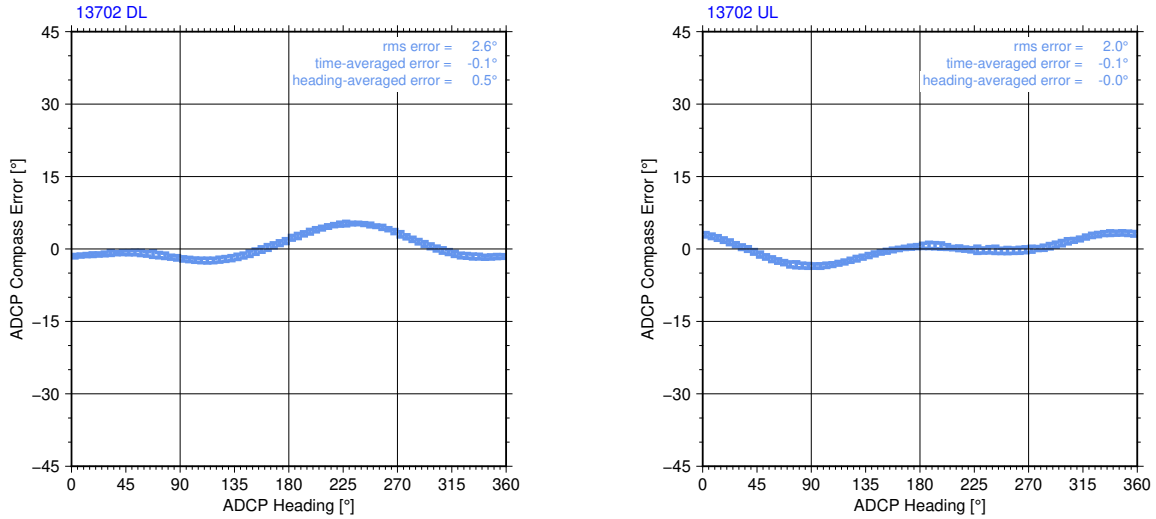


Figure 5: Heading dependent errors of the two ADCP compasses in an arbitrary profile. Discrepancies of such low magnitude indicate excellent calibration of both instrument compasses.

4 Horizontal Velocity QC

After the cruise, the available data from the IMP Mk3 (magnetometer and accelerometer, leg-2 only) were downloaded and processed as described by Thurnherr et al. (J. Tech., 2017), and the resulting replacement time series of pitch, roll and heading were merged with the raw ADCP data files, which are suitable for processing with standard software. There are no significant differences between the leg-2 profiles processed with the original data or with data from the IMP (not shown). Both the low sea state (Figure 4), resulting in comparatively weak pitching and rolling of the package, and the small compass errors, as evidenced by the small heading-dependent compass differences between the UL and DL instruments (Figure 5), contribute to this fact. For consistency all LADCP data from the P2 cruise were therefore processed and archived without IMP data.

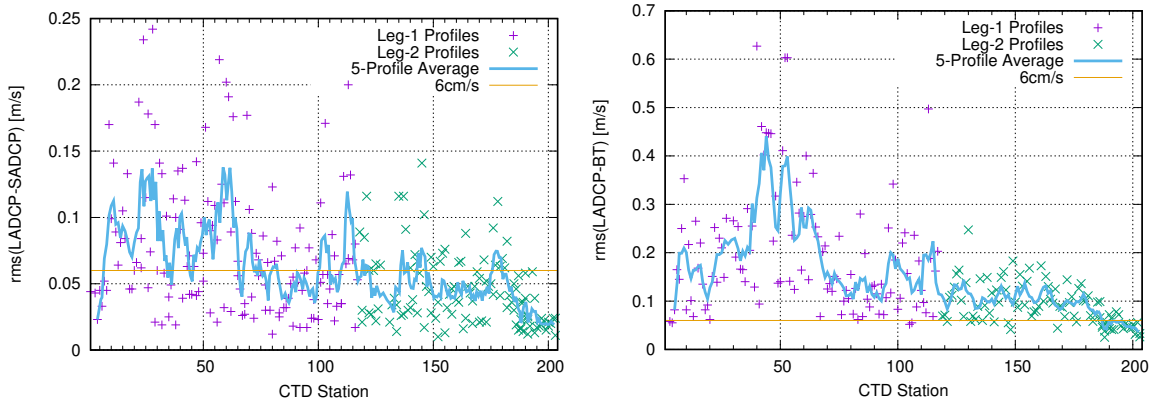


Figure 6: *rms* horizontal velocity differences, with low values indicating good agreement. (The horizontal lines indicate approximate empirical limits for high-quality profiles collected in regions of not-very-strong near-surface currents.) Note the different y-axis ranges in the two panels. Left panel: LADCP vs. SADCP velocities in the upper ocean. Right panel: LADCP vs. bottom-tracking velocities near the seabed.

The overall quality of the horizontal LADCP velocities is assessed by processing all profiles with the LDEO_IX implementation (version 15beta) of the velocity-inversion method without using the SADCP velocities to constrain the solutions, and then comparing the two independent velocity profiles in the upper ocean; Figure 6, left panel shows the profile-averaged *rms* velocity differences from this cruise. Based on data from many other cruises, high-quality LADCP profiles constrained with GPS and BT data typically agree with the corresponding SADCP velocities within $3\text{--}6\text{ cm}\cdot\text{s}^{-1}$ when averaged over a few profiles. In case of the P2 data, this is clearly not the case during most of leg 1, with the quality of the horizontal velocities gradually improving during the cruise. Because the low backscatter affects primarily the lower half of the profiles another, similar comparison was carried out between the “water-track” LADCP velocities and a set of bottom-tracked velocity profiles near the seabed. The velocity errors in this case are even greater, with only the profiles from the high-backscatter California Current System (Figure 3) passing the test (Figure 6, right panel).

Because of the low backscatter at depth along most of the P2 section (Figure 3) a visual assessment of all deep LADCP profiles was carried out by comparing the baroclinic (i.e. zero-vertical mean) meridional velocity profiles from the LADCP, processed with all available referencing constraints, to the two corresponding geostrophic estimates from the profiles bracketing the station position. Based on this assessment the profiles were assigned one of four quality levels, as illustrated with representative examples from leg 2 in Figure 7:

Level 1. Bad profiles, largely based on monotonic vertical-shear layers extending over 1000 m or more. The example profile in the top left figure panel is considered bad because neither of the geostrophic profiles is consistent with the monotonic large-scale LADCP shears between 2000 and 4000 m, and between 4000 and 5000 m. In particular the latter shear layer ($20\text{ cm}\cdot\text{s}^{-1}$ over 1000 m) is not realistic.

Level 2. Likely bad profiles. The example profile in the upper right figure panel is considered likely bad because neither of the geostrophic profiles is consistent with the unidirectional large-scale LADCP shear between 2300 and 4500 m. In contrast to the example shown in the upper left panel there are no individual shear layers that are unambiguously unrealistic.

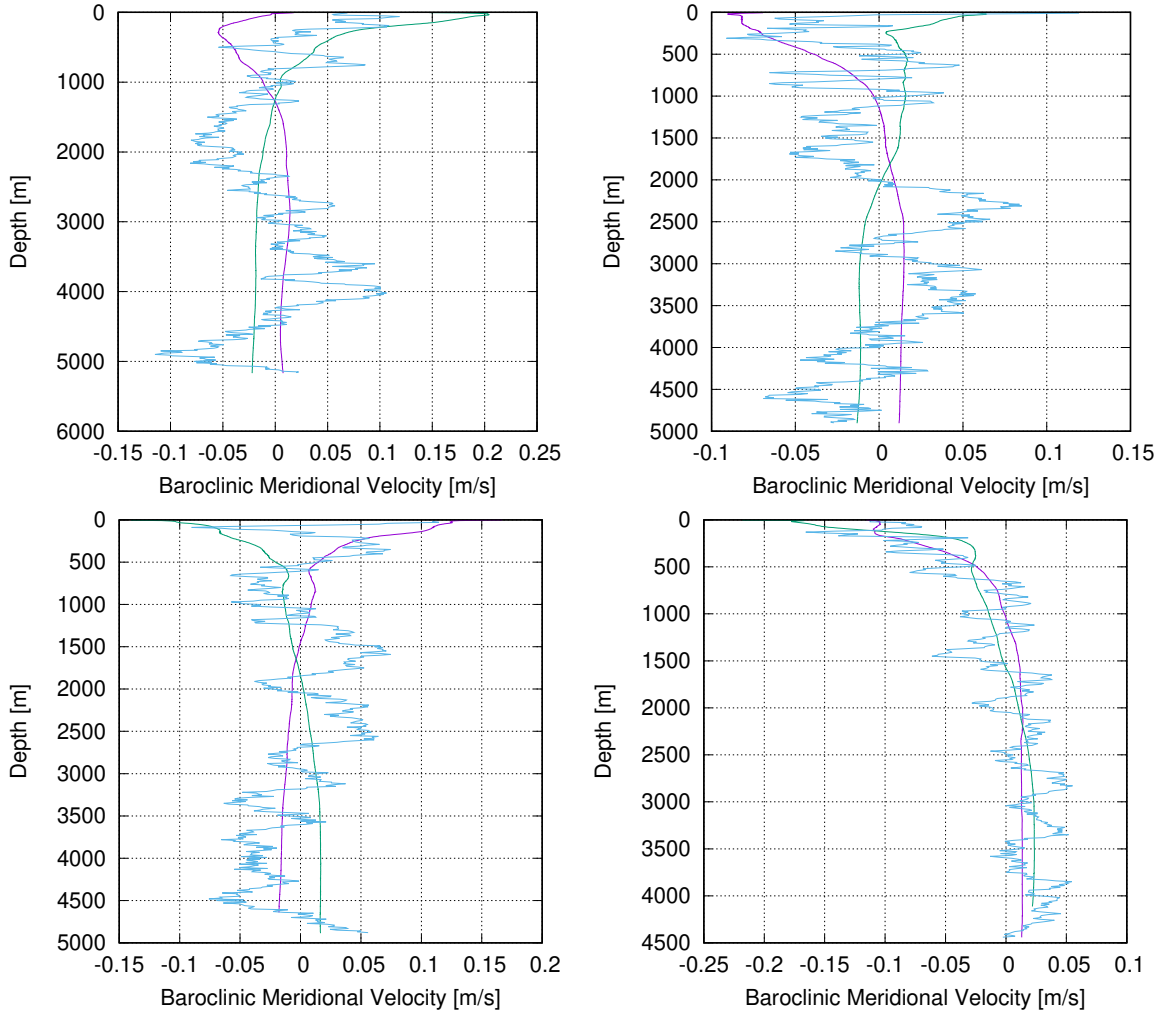


Figure 7: Example plots used for visually assessing the quality of the LADCP horizontal-velocity profiles; each plot shows the baroclinic meridional LADCP profile in blue, and the corresponding geostrophic velocities in the two adjacent station pairs in magenta and green. Clockwise from top left: bad profile; likely bad profile; likely good profile; good profile. See text for details.

Level 3. Likely good profiles. The example profile shown in the lower left figure panel agrees quite well with the geostrophic profiles, with the discrepancies limited to peak values about $5 \text{ cm} \cdot \text{s}^{-1}$ and with vertical scales of 500 m or less. There is considerable uncertainty, however, because of the mutual disagreement between the two geostrophic profiles.

Level 4. Good profiles. The example LADCP profile shown in the lower right figure panel shows good agreement with the two geostrophic profiles.

Out of the 88 deep (core) profiles of the P2 section, 36 (41%) are of low quality (levels 1 or 2). While the bad velocity data in the lower part of the water column prevent processing of the full-depth horizontal velocities using the ship-drift (GPS) constraint, the strong acoustic backscatter

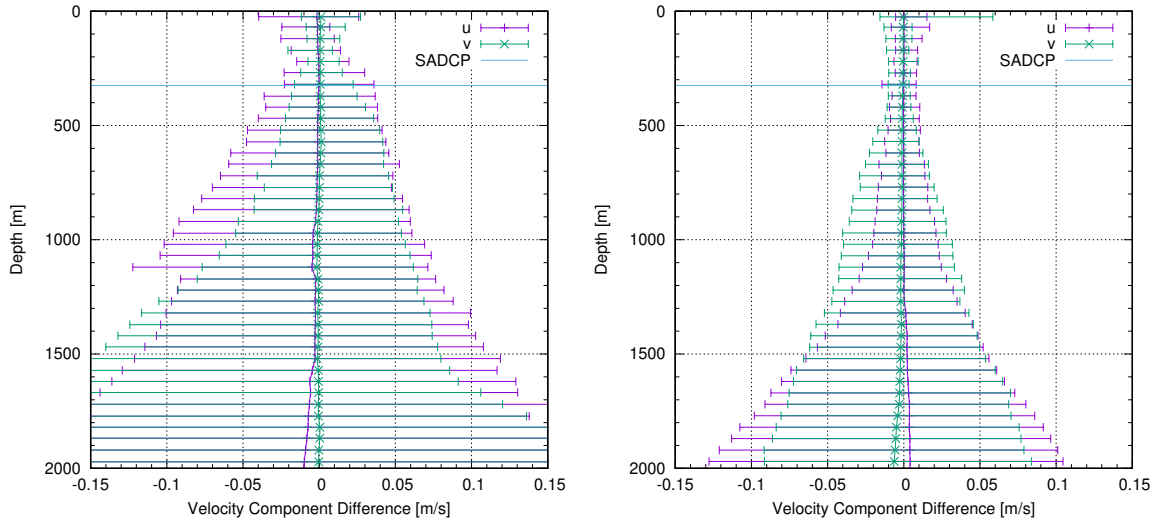


Figure 8: Mean profiles of velocity-component differences from the full-depth, high-quality profiles from (left) the first and (right) the second cruise leg; error bars indicate the 5% and 95% percentiles from bootstrapping; the horizontal blue lines indicate the depth of the deepest SADCPC velocities.

in the upper water column (Figure 3) is sufficient to constrain the vertical shear, allowing absolute upper-ocean LADCP profiles to be referenced with the SADCPC constraint alone. In order to quantify the velocity uncertainties for these profiles, velocity component differences were calculated between the fully constrained velocities and the velocities referenced only with the SADCPC constraint, using only the high-quality profiles. Figure 8 shows mean profiles of both velocity components from the two cruise legs. While the patterns are similar, due to the Kuroshio and its eddies the upper-ocean velocities from leg-1 were significantly stronger than the leg-2 velocities, accounting both for the larger error bars and the greater mean values. Therefore, leg-2 data are used to determine the cutoff depth for the upper-ocean profiles. Adding the velocity differences (uncertainties) near the bottom of the SADCPC constraint ($2 \text{ cm}\cdot\text{s}^{-1}$) to the nominal $3 \text{ cm}\cdot\text{s}^{-1}$ uncertainty for high-quality LADCP profiles (Thurnherr, J.Tech. 2010)) yields a limit of $5 \text{ cm}\cdot\text{s}^{-1}$ for the magnitude of the error bars, which implies that 1500 m is a suitable cutoff depth for the upper ocean profiles collected with insufficient backscatter at depth. Note that this implies that the SADCPC velocities provides a suitable constraint at vertical distances up to 1200 m from the constraint. With SADCPC data from a lower-frequency instrument the same method is expected to yield high-quality horizontal velocity profiles in regions of weak acoustic backscatter down to 2000 m or more.

Figure 9 shows sections of the high-quality zonal and meridional velocity from the LADCP system. In addition to the velocities shown in the figure, the deep profiles from the second crossing of the California Current System and all bio casts were collected in regions where the acoustic backscatter is strong (Figure 3) and their data quality is excellent throughout (not shown).

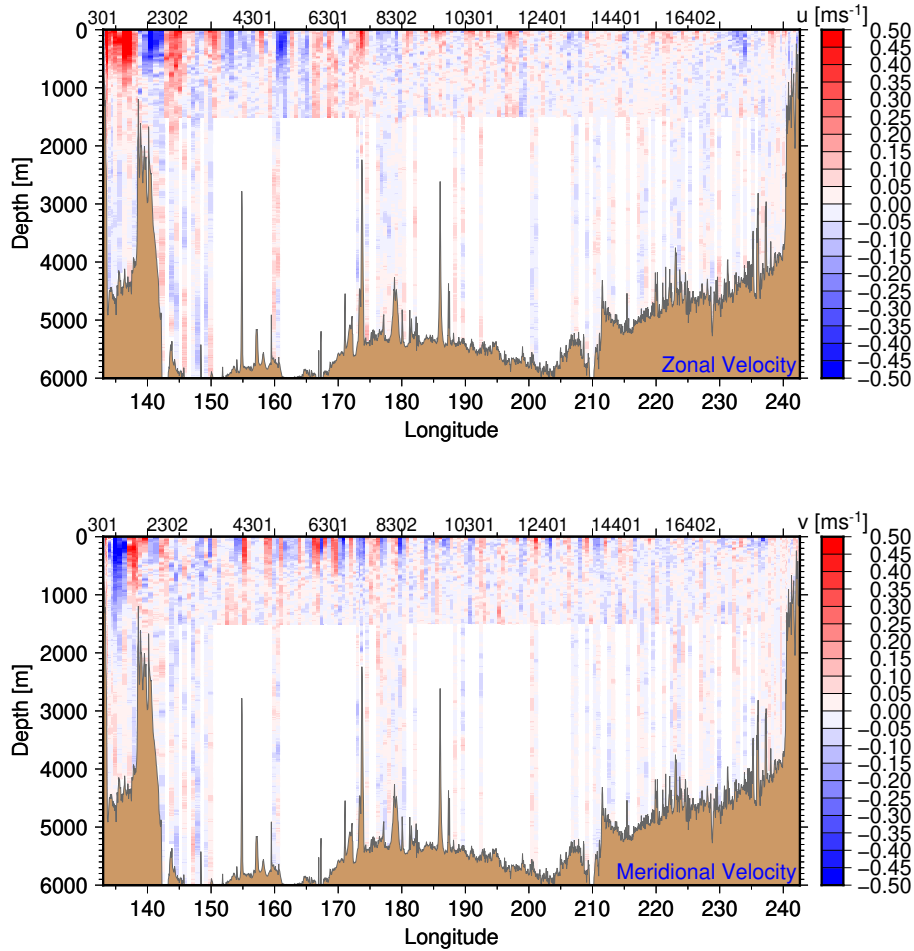


Figure 9: High-quality zonal (upper panel) and meridional (lower panel) velocities from the LADCP. See text for details.

5 Vertical Velocity QC

In order to process the LADCP data for vertical ocean velocity the LADCP_w software, version 2.1, was used. With two ADCPs measuring the vertical velocity field QC is based primarily on comparisons between the two largely independent¹ w measurements. In contrast to horizontal velocity, which can only be derived from full profile data, the effects of measurement errors due to insufficient backscatter, excessive instrument motion, etc., on vertical velocity are localized and can be removed during processing, causing gaps in the resulting profiles. Both example profiles shown in Figure 10 have gaps below 3500 m, although the downcast from profile 14801 is gap-free. In both profiles there is good agreement between the data from the two ADCPs outside the gaps, as indicated by the w

¹The same portion of the water column is sampled at different times by the two ADCPs. Only biases related to the CTD pressure measurements are common to the vertical velocity measurements from both instruments.

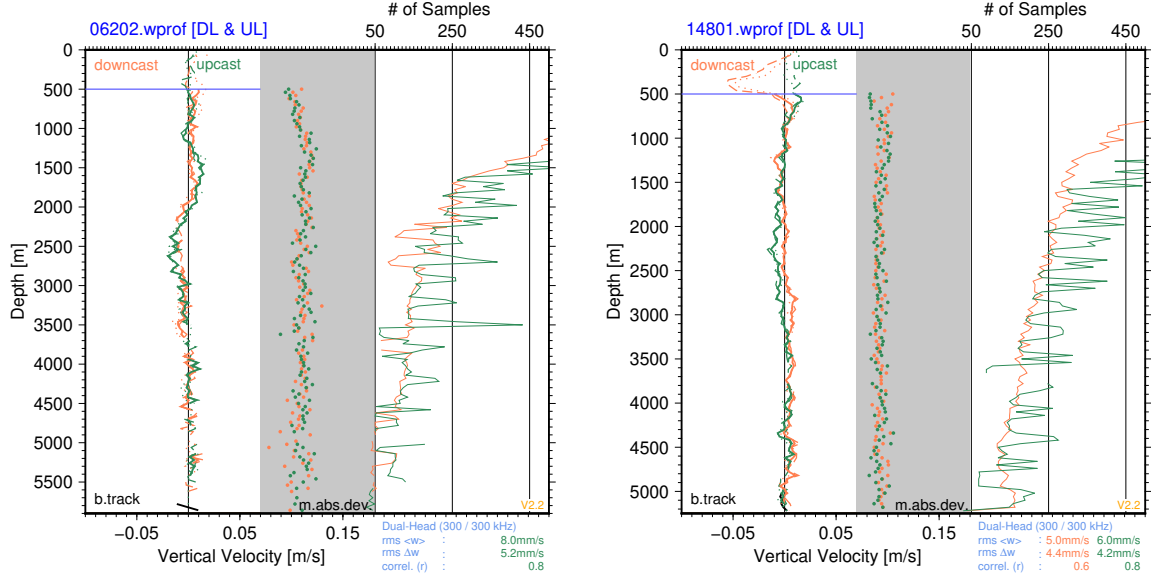


Figure 10: Diagnostic figures from two example vertical velocity profiles. Each panel shows (from left to right) vertical ocean velocity (dashed: DL, dotted: UL, combined: heavy; blue line indicates bottom of near-surface layer affected by biology), mean-absolute-deviation in each w bin (bullets) and number of samples in each bin (lines), as well as instrument type and profile-averaged w statistics (blue text in the bottom right corner).

correlation statistics printed in the figure panels. (There are too many gaps in the downcast data from profile 06202 for the correlation statistics to be reported.)

The downcast from profile 14801 shows a layer of strong apparent downwelling between 100 and 500 m, whereas the upcast velocities at the same depth are much weaker and qualitatively similar to the velocities below. The profile was collected at daybreak, with the downcast passing through 500 m before sunrise and the upcast several hours later. There are no apparent hydrographic anomalies in the CTD data from the same profile, nor is there any apparent horizontal velocity signal associated with the downwelling peak in the downcast. On the other hand, the downwelling peak was observed by both ADCPs independently, and we note that 500 m coincides closely with a prominent subsurface maximum of acoustic backscatter. Taken together, these observations suggest that the apparent negative w above 500 m during the downcast of this profile are more likely related to biological contamination (swimmers) than to downwelling of the water. Strong support for this inference is provided by a data set from the northeastern Gulf of Mexico where there are about a dozen profiles collected with either the downcast in daylight and the upcast at night or the other way round. Without exception, all those profiles show downwelling peaks similar to those in the P2 profile during darkness without any apparent w anomalies during daylight. Based on these observations, the most likely cause for the apparent downwelling are swimming organisms. (It is noted in this context that an ADCP cannot distinguish between horizontally homogeneous downwelling and radial horizontal motion away from the instrument. It is furthermore noted that due to the ADCP transducer geometry symmetric radial motion around the instrument does not project on the horizontal velocities.)

Biological contamination in the upper water column along P2 is not restricted to the example profile shown in the figure: Mean profiles of rms vertical velocity show strong (sharply defined)

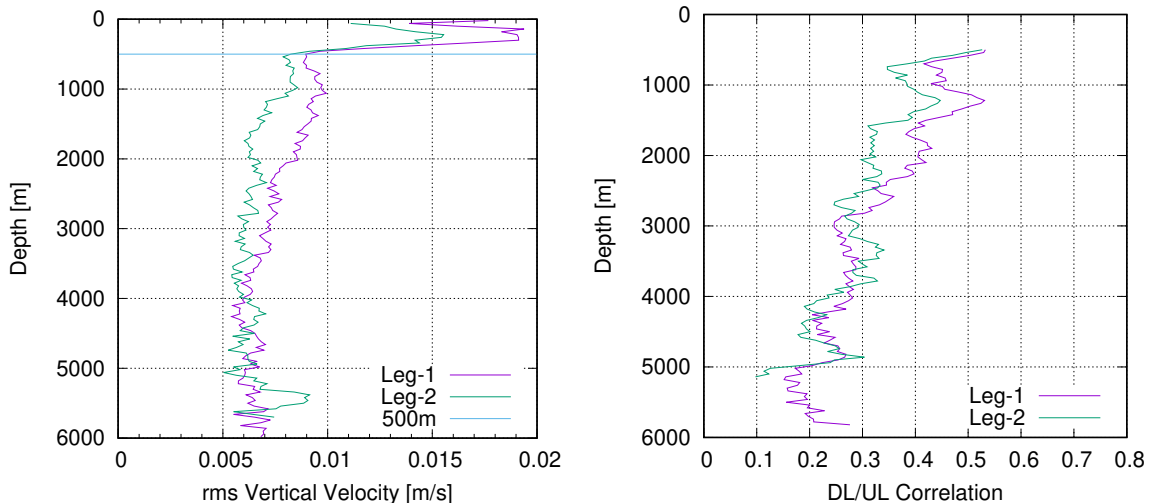


Figure 11: Left panel: Profiles of *rms* vertical velocity from the two cruise legs. Right Panel: Cruise-leg-average profiles of the correlation coefficients between the vertical-velocity measurements from the two ADCPs in 320 m-thick windows.

inflections near 500 m in the data from both cruise legs (Figure 11, left panel), with significantly elevated w above that depth. Mean CTD profiles show no indications for any physical interface at this level (not shown), which does, however, correspond closely with the depth of the subsurface backscatter maximum observed along most of the section (Figure 3). Based on these observations, the LADCP vertical velocity measurements from P2 above 500 m are assumed to be contaminated by biological activity and, therefore, not included in the archived data.

In order to quantify and visualize the quality of the vertical-velocity data, UL-DL correlation coefficients were calculated from the w measurements in 320 m-thick windows. These correlations are interpreted as a proxy for the signal-to-noise ratio of the w measurements, where the signal outside boundary layers is dominated by high-frequency internal gravity waves, and the noise is due to measurement errors. Where there are data from both instruments, the correlations between the UL and DL vertical velocities in the P2 data are mostly positive (Figure 12), indicating that the LADCP measurements are not dominated by instrument noise. Average profiles of the UL/DL correlation coefficient from the two cruise legs indicate that there are clear spatial patterns in the signal-to-noise ratio of the w measurements (Figure 11, right panel). The weakening of the correlations with increasing depth seen in both cruise legs is qualitatively consistent both with the buoyancy-scaling of internal wave motion, which is also reflected in the profiles of *rms* vertical velocity (left figure panel), and with increased measurement noise in regions of weak acoustic backscatter. The differences between the mean correlation coefficients above 3500 m from the two cruise legs are more likely dominated by differences in internal-wave levels than by the higher levels of acoustic backscatter observed during leg-1, on the other hand (not shown). Taken together the correlations between the vertical velocities from the two ADCPs indicate that the data quality of the full depth w profiles is very good, including the profiles collected in regions of weak acoustic backscatter.

The LADCP_w software includes the LADCP_VKE tool, which is used to estimate vertical kinetic energy (VKE) and, implementing a finescale parameterization based on high-frequency internal waves, kinetic energy dissipation ϵ_{VKE} (for details, see Thurnherr et al., GRL 2015). When applied to the P2 data this parameterization results in physically reasonable patterns (Figure 1). In particular,

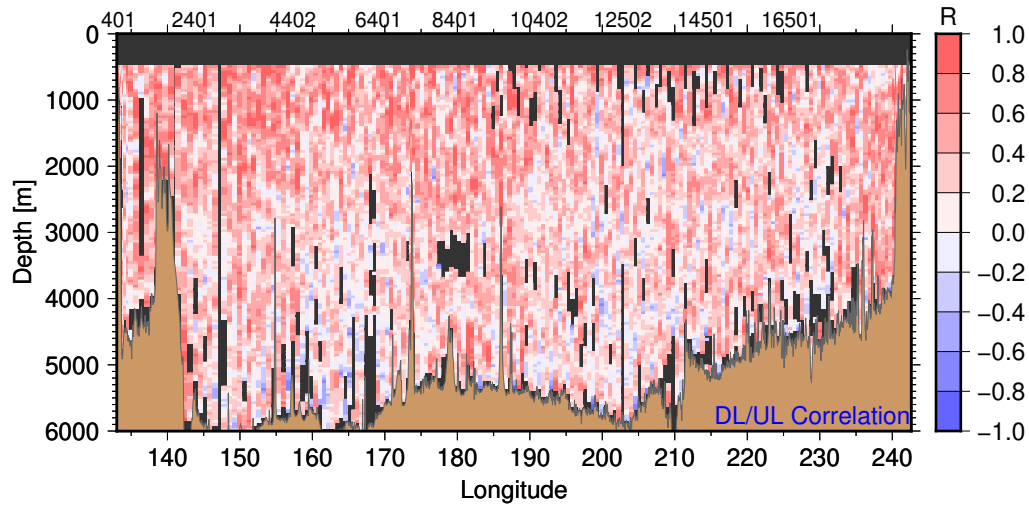


Figure 12: Downcast/upcast average correlation coefficients between the vertical-velocity measurements from the two ADCPs in 320 m-thick windows; a minimum of 6 samples are required for each correlation. Regions without data from both instruments are shaded dark. As discussed in the text, many of the low/negative correlation coefficients are related to low signal, rather than to measurement problems.

parameterized turbulence levels are regionally different, with particularly high and low levels in the Kuroshio region and in the California Current System, respectively.